Biosensors and Bioelectronics 26 (2011) 2390–2395

Contents lists available at ScienceDirect

Biosensors and Bioelectronics

journal homepage: www.elsevier.com/locate/bios

Ultrasensitive quantum dots-based DNA detection and hybridization kinetics analysis with evanescent wave biosensing platform

Feng Long, Shuxu Wu, Miao He, Tiezheng Tong, Hanchang Shi*

Environmental Simulation and Pollution Control State Key Joint Laboratory, Department of Environment Science and Engineering, Tsinghua University, Beijing 100084, China

ARTICLE INFO

Article history:
Received 8 August 2010
Received in revised form 10 October 2010
Accepted 11 October 2010
Available online 16 October 2010

Keywords:
DNA
Quantum dots
Evanescent wave biosensor
Hybridization kinetics

ABSTRACT

Ultrasensitive DNA detection was achieved using a new biosensing platform based on quantum dots (QDs) and total internal reflection fluorescence, which featured an exceptional detection limit of 3.2 amol of bound target DNA. The reusable sensor surface was produced by covalently immobilizing streptavidin onto a self-assembled alkanethiol monolayer of fiber optic probe through a heterobifunctional reagent. Streptavidin served as a versatile binding element for biotinylated single-strand DNA (ssDNA). The ssDNA-coated fiber probe was evaluated as a nucleic acid biosensor through a DNA–DNA hybridization assay for a 30-mer ssDNA, which were the segments of the uidA gene of *Escherichia coli* and labeled by QDs using avidin–biotin interaction. Several negative control tests revealed the absence of significant non-specific binding. It also showed that bound target DNA could easily be eluted from the sensor surface using SDS solution (pH 1.9) without any significant loss of performance after more than 30 assay cycles. A quantitative measurement of DNA binding kinetics was achieved with high accuracy, indicating an association rate of 1.38×10^6 M^{-1} s^{-1} and a dissociation rate of 4.67×10^{-3} s^{-1}. The proposed biosensing platform provides a simple, cheap, fast, and robust solution for many potential applications including clinical diagnosis, pathology, and genetics.

1. Introduction

Highly-sensitive, rapid, and reliable detection of DNA/RNA without expensive instrumentation and extensive sample pretreatment, is in great demand for clinical diagnosis, pathology, and genetics. Among the various detection schemes currently under investigation, optical fiber biosensors based on total internal reflection fluorescence (TIRF) have shown great potential in providing viable solutions to these challenges (Abel et al., 1996; Leung et al., 2007). When optical fiber transmits light on the basis of the principle of total internal reflection, the evanescent wave penetrates essentially into the surrounding cladding of lower refractive index and exponentially decays with distance. The evanescent wave can excite fluorescence primarily from the fluorescent labeled analyte complexes bound to the surface through affinity recognition interactions. The signal changes over time are directly related to the binding kinetics of biomolecular interactions (Golden et al., 1997). Knowledge on hybridization kinetics at a solid-phase interface is critical for the design and optimization of biosensing techniques and the efficient collection of genomic information (Zeng et al., 2003). In addition, quantum dots (QDs) have become powerful tools for biosensing and medical imaging because of their unique optical properties, such as high quantum yield, photostability, narrow emission spectrum, and broad absorption (Michalet et al., 2005; Resch-Genger et al., 2008). Compared with organic dyes, QDs are 20 times brighter and several orders of magnitude more photostable (Chan and Nie, 1998; Sukhanova et al., 2004). The combination of the evanescent wave biosensor and QDs can be used for ultrasensitive DNA detection and analysis of hybridization kinetics at solid interfaces.

This study is the first to propose an all-fiber DNA biosensing platform based on QDs and TIRF. Compared with conventional fiber optic DNA biosensors that need numerous optical components with stringent optical alignment requirements, the proposed DNA biosensor shows considerable promise in obtaining sequence-specific information in a simple, fast, and portable technology. *Escherichia coli* is selected as a model pathogen to validate the detection capabilities of the developed biosensor using QD-DNA as reporter molecules. The interfacial hybridization behaviors of DNA on the sensor surface are determined in real-time, and kinetic parameters are calculated based on the proposed theory.

2. Experimental

2.1. Chemicals and reagents

Ovalbumin (OVA), bovine serum albumin (BSA), 3-mercaptopropyl-trimethoxysilane (MTS), N-(4-maleimidobu-

* Corresponding author. Tel.: +86 10 62773095; fax: +86 10 62771472.
E-mail address: hanchang@mail.tsinghua.edu.cn (H. Shi).

0956-5663/$ – see front matter © 2010 Elsevier B.V. All rights reserved.
doi:10.1016/j.bios.2010.10.018

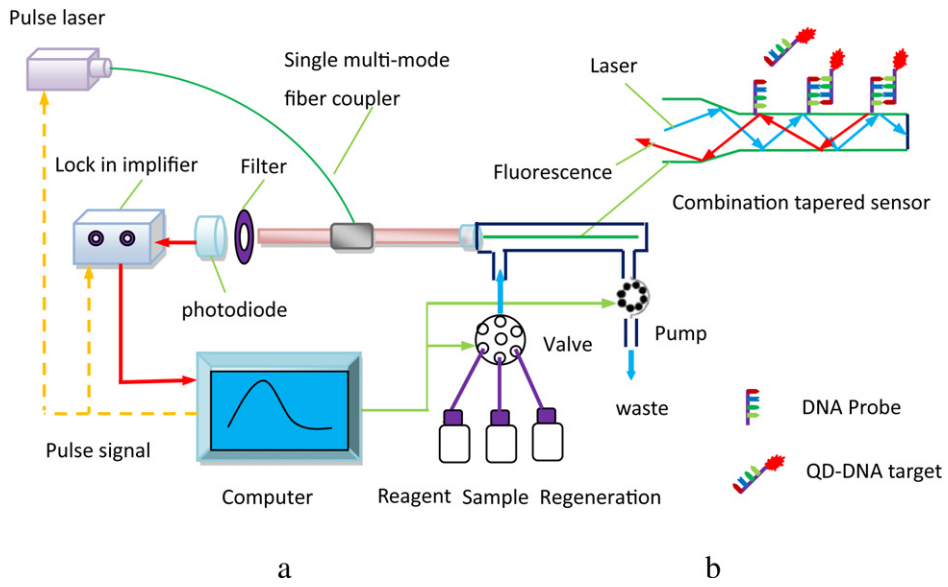

Fig. 1. (a) Schematic diagram of the structure of evanescent wave DNA biosensor and (b) schematic diagram of combination-tapered fiber sensor and mechanical schematic of DNA detection.

tyryloxy) succinimide (GMBS), and 1-ethyl-3-dimethylaminopropyl carbodiimide hydrochloride (EDC) were purchased from Sigma–Aldrich (Germany). The Qdot® streptavidin conjugates (Q10161MP) were obtained from Invitrogen Ltd. (USA). DNA oligonucleotides used were the segments of the uidA gene of *E. coli*, which were supplied by Takara Biotechnology (Dalian) Co. (China). The following oligonucleotide were used: DNA probe, 5′-biotin-TTTTTTTTTTACGCTCACACCGATACCATC-3′; perfectly matched cDNA (PM), 5′-biotin-AGTCTCAGCAGATGGTATCGGTGTGAGCGT-3′; non-complementary DNA (NM), 5′-biotin-AGTCTCAGCAAG-TCTCAGCAAGTC TCAGCA-3′; one-base mismatched cDNA (MM), 5′-biotin-AGTCTCAGCAGATG GTAGCGGTGTGAGCGT-3′, a perfectly matched cDNA labeled by Dylight 680 (Dyl-PM), 5′-Dylight680-AGTCTCAGCAGATGGTATCGGTGTGAGCGT-3′. All oligonucleotides were purified by reverse-phase high performance liquid chromatography (RP-HPLC) to remove failure sequences that interfere in the experiments. A biotin-tethered oligonucleotide stock solution was prepared with 10 mM phosphate buffered solution (PBS, pH 7.4) containing 1 mM EDTA; the stock solution was kept frozen afterwards. The PM, NM, and MM target oligonucleotides were dissolved in TE buffer (10 mM Tris–HCl, 1 mM EDTA, pH 7.4) and kept frozen for storage. All solutions were prepared with ultrapure water from a Millipore Milli-Q system. All other reagents, unless specified, were purchased from the Beijing Chemical Agents (China). All chemicals were of analytical reagent grade.

2.2. Evanescent wave biosensing platform

Fig. 1 presents the schematic of the proposed QDs-based DNA biosensor. Due to the light absorption efficiency of Qdot® nanocrystals used increased dramatically to the blue of the emission (Chan and Nie, 1998; Michalet et al., 2005), the 405-nm pulse diode laser (HuayuanStar Ltd., China) with pigtail acted as the excitation light source. The laser entered from the single multi-mode fiber into the single-multi mode fiber coupler (Beijing Glass Research Institute, China) with a diameter of 600 μm and a numerical aperture of 0.22. Excitation light from the laser was coupled to the fiber-based DNA sensor through a fiber connector. Incident light was propagated along the length of the fiber probe via total internal reflection. The evanescent wave was generated at the surface of the probe and decayed exponentially with distance. It excited the fluorophores labeled in the surface-bound analyte complex. Part of the fluorescence coupled back into the fiber sensor was subsequently filtered by a bandpass filter (FF01-692/40, Semrock, USA), and detected by photodiodes through a digital lock-in amplifier produced in the laboratory. In this system, both the transmission of the excitation light and the collection and transmission of fluorescence were achieved by fiber optics with a single-multi mode fiber optic coupler (Long et al., 2008a). In this way, the optical components required were reduced, and the need for frequent optical alignment became rare. The DNA biosensor is embedded in a flow glass cell (Ø2 × 40 mm, 200 μL) with an inlet and an outlet. The flow cell is attached via Tygon® tubing with an inner diameter of 0.76 mm to a peristaltic pump, which controlled the flow rate and delivered various solutions. Buffer, sample solutions, and regeneration solutions could be exchanged through the six-way valve. Control of the pump and six-way valve, as well as performing data acquisition and processing were automatically performed by a computer. The computer also provided pulse signals of the same frequency for the laser and for the lock-in amplifier.

2.3. Single-strand DNA (ssDNA) labeled with QDs

Biomolecules can be attached either covalently or non-covalently on the surface of QDs. Avidin–biotin cross-linking, one of the most popular methods for conjugating biomolecules on the surface of QD, was used to label DNA with QDs. All biotinylated target DNA were labeled by the QD-streptavidin conjugate as follows: 100 μL of 10 μM biotinylated DNA were added into 2 μM QD-streptavidin conjugate solution and the mixture was stirred gently for 20 min to allow for streptavidin and biotin to bind. Then, to remove any excess unbound biotinylated cDNA, the solution was centrifuged at 2000 rpm in the ultrafiltration unit for at least five buffer exchanges (50 mM borate buffer, pH 8.3). The QD-DNA conjugate solution was stored at 4 °C until use.

2.4. Modification of optical fiber sensor

A combination-tapered fiber optic sensor was prepared as described previously (Long et al., 2008b). The modification method used to immobilize DNA probe onto the sensor surface is shown in Fig. 2. Combination-tapered fiber sensor was initially cleaned with

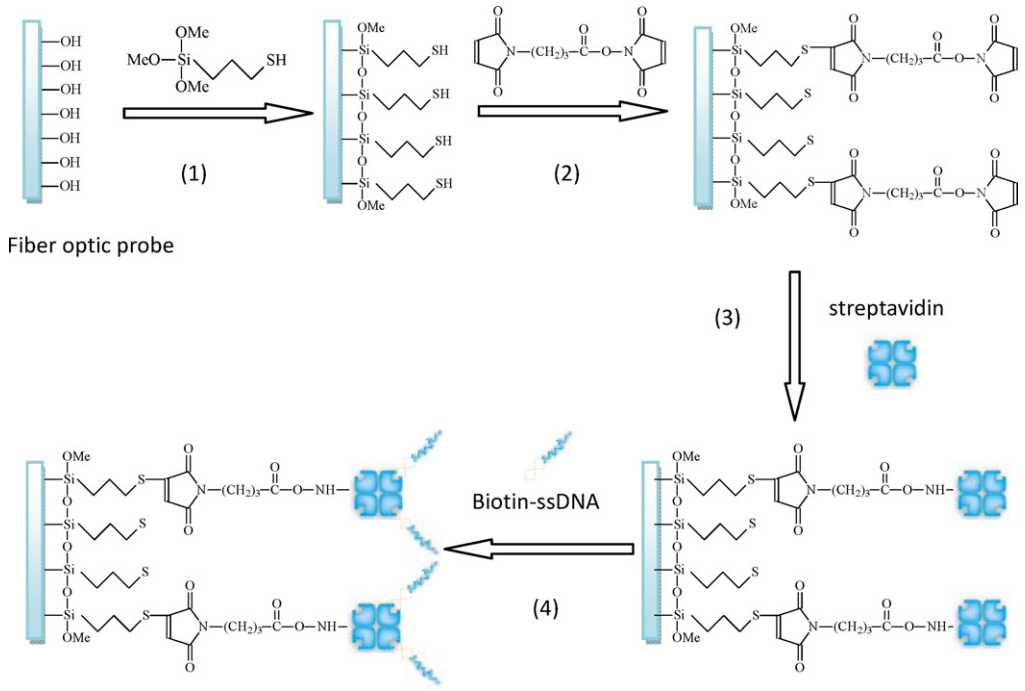

Fig. 2. Schematic of optical fiber sensor modification. Firstly, the hydroxyl groups on the probe surface were covalently attached with MTS molecules (step 1). Secondly, the thiol group of silane reacted with the maleimide function of the bifunctional cross-linker GMBS (step 2). Thirdly, the ester moiety of the GMBS allowed the covalent linking of the streptavidin through an amino group (step 3). Finally, biotinylated ssDNA probes were attached to the immobilized streptavidin (step 4).

Piranha reagents (concentrated H_2SO_4/H_2O_2 2:1), rinsed with distilled deionized water, and dried in N_2. The probe was then placed in 2% MTS in toluene for 2 h, under an inert atmosphere. Excess MTS was eliminated with dry toluene to assure the order and uniformity of the self-assembled monolayer. The thiol group of silane was allowed to react for 1 h with a heterobifunctional cross-linker, 2 mM GMBS in ethanol. After rinsing with ethanol and PBS, the succinimide group on GMBS was then incubated with streptavidin for 2 h to covalently bind with its epsilon amino groups. Then, 0.5 μM biotinylated ssDNA probe was attached to the immobilized streptavidin for 20 min. After rinsing with PBS, immersion of the fiber sensor in 2 mg/mL BSA was then carried out for 30 min to block non-specific absorption sites.

2.5. DNA hybridization detection and regeneration

The sensor surface was washed with hybridization buffer (20 mM Tris–HCl, pH 8.0, 0.5 M $MgCl_2$). The PM, NM, and MM oligonucleotides labeled by QDs or Dyl-PM oligonucleotides were delivered into the sample cell, respectively. Real-time monitoring of fluorescence signals was performed as hybridization occurring between the DNA probe immobilized onto the sensor surface and the target DNA in the solution. For the regeneration of active sensor surface, 0.5% SDS solution (pH 1.9), 10 mM NaOH solution, and 10 mM HCl solution were used to break the DNA duplex, respectively.

3. Results and discussion

3.1. Immobilization of DNA probe

Avidin–biotin binding is one of the most common methods for DNA immobilization onto a solid surface (Ebersole et al., 1990). In this study, immobilization of the DNA probe included a few important steps (Fig. 2): silanization to add thiol groups (–SH) to the surface, conjugation between the thiol groups and the epsilon amino group of streptavidin with a heterobifunctional cross-linker, GMBS, and coupling biotinylated ssDNA probe to the streptavidin-modified surface. Using this method, the biotinylated ssDNA probe can be immobilized onto the sensor surface just before use. This prevents possible DNA damage during storage and maintains maximum activity. In addition, the sensor surface modified by streptavidin–biotin binding, completed within a few minutes, was stable and reusable. When DNA is attached to a solid surface with a spacer connected to one of the ends of the nucleic acid chain, the spacer can lead to DNA molecular flexibility (Fang et al., 1999). Therefore, a 10-dT spacer was added between biotin and the DNA probe to reduce steric hindrances for DNA hybridization.

Because the density of the DNA probe immobilized onto the surface of a solid substrate may affect the electrostatic properties and local ionic strength of the surface, it plays an important role in hybridization kinetics, efficiency and selectivity (Watterson et al., 2000; Zeng et al., 2003). Previous studies indicated that the concentration of streptavidin immobilized onto a sensor surface by the modification method used here was about 0.45 pmol/cm^2 (Bhatia et al., 1989; Tedeschi et al., 2003). Assuming that the two biotin–DNAs were bound to each streptavidin on average, the surface density of the DNA probe was estimated to be 0.9 pmol/cm^2 (5.6×10^{11} probe molecules/cm^2), and the area occupied by each DNA strand was approximately 210 nm^2. In this low surface density regime, ssDNA strands had almost no interaction with each other considering that the 30-mer DNA probes were <11 nm in length (DNA base distance ~0.34 nm). This led to a high hybridization efficiency and fast binding kinetics (Peterson et al., 2001).

3.2. DNA hybridization detection

To perform hybridization assays, 1 nM of various DNA targets, such as perfectly matched cDNA (PM), one-base mismatched cDNA (MM), and non-complementary DNA (NM), was separately delivered over the sensor surface. Fig. 3a shows the typical fluorescence time trace during a complete hybridization process, which dis-

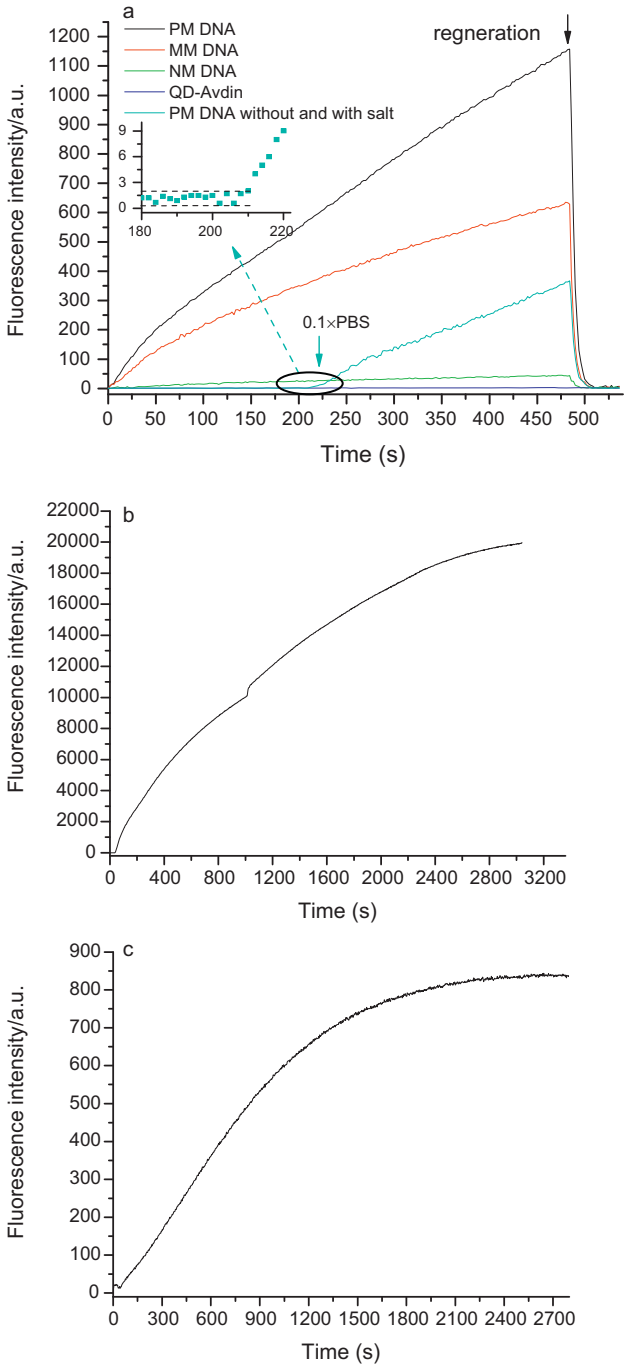

Fig. 3. (a) Typical signal trace observed in the flow of various target DNA solutions over the sensor surface. The inset shows a magnified view used to estimate signal noise. Dashed lines indicate standard deviations from the mean fluorescence signal value before binding. (b) and (c) Represents the fluorescence signal curves of 20 nM QD-DNA and 20 nM Dyl-DNA hybridization with the probe DNA immobilized onto the sensor surface, respectively.

played the dynamic process of the affinity interaction between the probe and the DNA target sequence. The PM oligonucleotide resulted in significantly increased fluorescence intensity, which was the highest among the targets. When MM oligonucleotide was used, a smaller increase in fluorescence intensity was observed. Whereas, there was no obvious fluorescence intensity for NM oligonucleotide. To re-confirm that the observed fluorescence signal was from specific DNA hybridization and not from non-specific adsorption or excitation of free QD-DNA in solution, the other two control experiments were also carried out: (1) The conjugate QD-streptavidin (5 nM) without any target DNA attached was placed in the sample cell, and no detectable fluorescence signal was observed. (2) The QD-DNA conjugate solution (1 nM) containing no salt was delivered over the sensor surface and no fluorescence signal was detected, suggesting that no hybridization had taken place. However, upon adding 0.1 × PBS to the QD-DNA conjugate solution, a significant fluorescence signal was observed, confirming that DNA hybridization did take place. DNA duplex formation strongly depended on the presence of salt which shields the strong electrostatic repulsion from the negatively charged phosphate backbones of DNA (Zhou et al., 2008). Therefore, the observed fluorescence signal was due to the specific hybridization between the QD-DNAs and the probe, and not from non-specific adsorption of QD-DNA on the sensor surface or from excitation of free QD-DNA in the solution.

Fig. 3b and c presents a plot of the fluorescence intensity as a function of time when 20 nM QD-PM and Dyl-PM oligonucleotides were delivered over the sensor surface, respectively. QD-PM and Dyl-PM were excited by a 405-nm or 635-nm pulse laser at the same power, respectively. In agreement with an earlier report (Chan and Nie, 1998), more than 20-fold increase in fluorescent signal was observed with the use of QD-PM compared with Dyl-PM. This was mainly due to the higher quantum yield and resistance to QDs' photobleaching. The platform of fluorescence signal could be obtained more quickly using Dyl-PM than QD-PM. This was because the laser was kept on throughout the whole detection period, and fluorescence was excited continuously during binding. The actual fluorescence intensity was an overlay of fluorescence excited from the labeled target DNA bound to the surface and from the degradation of bound fluorophores due to photobleaching and dissociation. The fluorescence signal increased as long as the binding rate of target DNA in solution was higher than the dissociation and photobleaching rates of the bound fluorophores. Then, it reached a maximum and decreased when the photobleaching and dissociation rates exceeded the rate of binding to the surface. Due to the high anti-photobleaching properties of QDs, the fluorescence signal for QD-PM increased until the real equilibrium binding was nearly achieved. It also indicated that the hybridization kinetic obtained using the quantum dots labeled DNA should be closer to the actual kinetic of DNA hybridization on the solid-phase surface than that obtained using organic dye-labeled DNA.

3.3. Hybridization kinetic assay

Before the discussion of the hybridization kinetics, we focus on the total fluorescence signal detected by the evanescent wave biosensor, which is composed of two components:

$$I_t = I_0 + I_h \quad (1)$$

where I_t is the total fluorescence intensity, I_0 is the background baseline intensity and contributions from other non-binding events, and I_h is the contribution from the hybridization of QD-DNA on the surface. From above discussion, the contribution of the fluorescence signal from non-specific adsorption could be negligible.

To measure hybridization kinetics and equilibrium constants, the resulting fluorescence signals were analyzed theoretically using the Langmuir model, which is a commonly accepted model for duplex formation in the presence of low probe density regimes (Fisher et al., 1994; Myszka, 1997; Peterson et al., 2002). The Langmuir model assumes that all binding sites are equivalent, that already occupied sites do not influence the binding reaction of adjacent sites, and that the surface is homogenously covered by monolayers. Thus, hybridization binding between immobilized

probe (P) and the target DNA (T) in solution can be described by

$$T + P \underset{k_{off}}{\overset{k_{on}}{\rightleftharpoons}} T:P \quad (2)$$

where T:P is the target–probe complex, k_{on} is the association rate constant, and k_{off} is the dissociation rate constant. The resulting time dependent surface coverage Θ can be described by

$$\frac{\partial \Theta}{\partial t} = C_0 \cdot k_{on}(1 - \Theta) - k_{off}\Theta \quad (3)$$

where C_0 is the concentration of the target DNA in solution. At the outset of hybridization, the forward rate is at the maximum, and the reverse rate and Θ are zero. The surface will be occupied until all binding sites are blocked. Since the fluorescence signal (I) is proportional to Θ, Eq. (3) can be expressed as

$$\frac{\partial I}{\partial t} = C_0 \cdot k_{on}(I_{max} - I) - k_{off}I \quad (4)$$

$$\frac{\partial}{\partial I}\left(\frac{\partial I}{\partial t}\right) = -k_{on}C_0 - k_{off} \quad (5)$$

where I_{max} is the maximum fluorescence signal when the DNA probe of the sensor surface is saturated by the target DNA sequence. From Eq. (5), the linear relationship between $\partial/\partial I(\partial I/\partial t)$ and the concentration of fluorescence-labeled DNA was measured. k_{on} and k_{off} are obtained simultaneously by the slope and intersection of the linear response in Eq. (5).

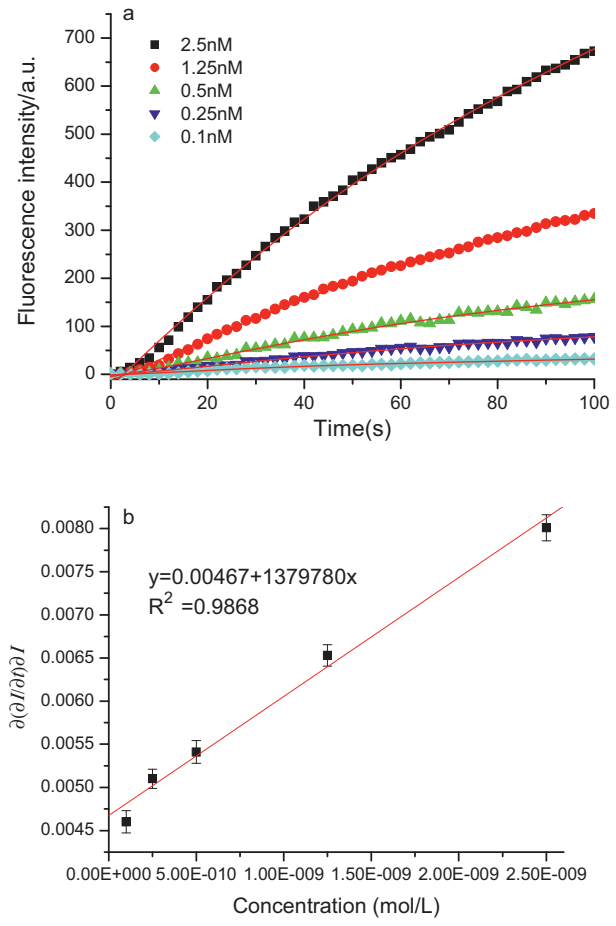

Fig. 4. (a) Typical kinetic curves representing the molecular interactions on the sensor surface. After a short background measurement, the association phase was observed by introducing the target to the probe immobilized on the sensor surface. The surface was regenerated by SDS solution (pH 1.9) and (b) determination of binding kinetics for DNA hybridization.

In the case of efficient transport, the hybridization process is reaction-limited, Eq. (4) can readily be solved.

$$\frac{I(t)}{I_{max}} = \frac{K_A C_0}{1 + K_A C_0}(1 - e^{-(k_{on}C_0 + k_{off})t}) \quad (6)$$

where $K_A = k_{on}/k_{off}$ is the equilibrium association constant.

Fig. 4a shows the time response of fluorescence intensity from hybridization binding between DNA probe and target QD-DNA of various concentrations in the range of 0.1–2.5 nM. For QD-DNA, the linear equation was obtained as $y = 1{,}379{,}780x + 0.00467$ ($R^2 = 0.9868$) in Fig. 4b. The association rate constant $k_{on} = 1.38 \times 10^6\ M^{-1}\ s^{-1}$ and the dissociation rate constant $k_{off} = 4.67 \times 10^{-3}\ s^{-1}$ were obtained using Eq. (5). Thus, the equilibrium association constant ($K_a = 2.96 \times 10^8\ M^{-1}$) was obtained from the interaction of the probe and the target DNA. This is in agreement with earlier data obtained using different methods for DNA/DNA hybridization, such as $4.98 \times 10^8\ M^{-1}$ (15-mer) and $2.62 \times 10^8\ M^{-1}$ (75-mer), which was obtained from a surface plasmon diffraction sensor (Yu et al., 2004), $5.7 \times 10^8\ M^{-1}$ (20-mer) obtained from a quartz crystal microbalance microbalance (Okahata et al., 1998), and $1.47 \times 10^8\ M^{-1}$ (19-mer) obtained from electrochemical impedance spectroscopy (Li et al., 2007). Thus, the simple setup presented here could provide an alternative technique in characterizing biomolecular interactions in many applications.

3.4. Sensitivity of DNA biosensor

High sensitivity is critical for developing a new biosensor or microarray with excellent performance. The limit of detection of biosensors is usually defined as three times standard deviation of the mean blank values. That is to say, the detection limit is the minimal target concentration in solution that generates a signal-to-noise ratio of 3. Thus, a titration experiment using QD-DNA as target was performed. When the reaction time was 30 min, a significant fluorescent signal was observed at 1 pM. When the target DNA concentration was lower, a longer reaction time was needed to get a measurable fluorescent signal. Hence, the detection limit for QD-DNA hybridization with was below 1×10^{-12} M.

However, the detection limit obtained above depends on the diffusion limit of DNA in solutions and the intrinsic binding affinity of oligonucleotides. It does not necessarily reflect the intrinsic sensor characteristics (Rant et al., 2007). Another criterion that is frequently used to measure sensitivity is the minimal amount of surface-bound target required to generate a sensor response. The hybridization yield was assumed to be 100%, which is reasonable when the low probe density is used (Peterson et al., 2001). With respect to the amount of bound target with QD-DNA binding trace (Fig. 3a), a 0.5% occupation of the available binding sites on the DNA capture layer was estimated to result in a measurable sensor response. This was done by comparing the signal noise to the change in fluorescence signal under saturation conditions. With an effective sensor area at 3.45 mm^2 and a surface density of 5.6×10^{11} molecules/cm^2, the sensor sensitivity was estimated to be 3.2 amol (3.2×10^{-18} mol) of the target DNA. Commercially available label-free sensors, such as surface plasmon resonance or quartz crystal microbalance sensors, have detection limits of >20 and >2000 amol of bound protein, respectively (Rant et al., 2009). Further optimization of the system is possible by increasing the sensitivity of the photodiode and lock-in amplifier, which may reduce the detection limit to <1 amol.

3.5. Regeneration of sensor surface

Regeneration of a surface-immobilized probe without a significant loss of hybridization activity is a desired feature of biosensors for practical applications. A number of strategies have been inves-

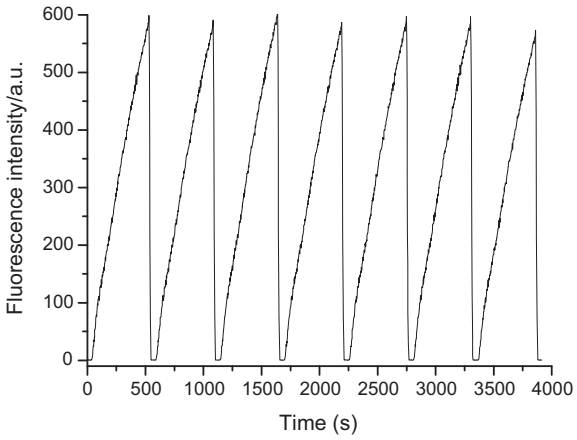

Fig. 5. Maximum signal and representative response curves for DNA hybridization using the proposed biosensor in multiple cycles when the concentration of the target DNA is 0.6 nM. The sensor surface was regenerated with SDS solution at each cycle.

tigated for the regeneration of a DNA sensor including thermal techniques, addition of strong acid or base, use of urea, and so on (Gao et al., 2006; Sassolas et al., 2008; Zhang et al., 2009). Considering that the avidin layer might be destroyed at high temperatures, chemical methods were used in this study to regenerate the evanescent wave DNA biosensor.

To evaluate the stability and activity of the immobilized surface of the DNA probe, a number of target DNA association/dissociation cycles were monitored for this same surface after regeneration with SDS solution (pH 1.9) and rehybridization. Seven continuous measurement cycles are performed in Fig. 5. Actually, the immobilized recognition element was found to retain at least 30 successive assays, without any significant loss of performance (less than 8% decrease). After each DNA determination cycle, a complete removal of non-covalently bound target DNA was achieved within several seconds, and the active sensor surface was regenerated with SDS solution. Results also showed that the complete regeneration of sensor surface could not be achieved with 10 mM NaOH or HCl, which was unlike those found in previous reports (Sassolas et al., 2008; Zhang et al., 2009).

4. Conclusion

In summary, a method with a new all-fiber based biosensing platform has been developed for the ultrasensitive DNA detection and hybridization kinetics assay. The achieved ultrasensitivity benefits from the exceptional optical properties of QD and from the advantages of the evanescent wave technique. The regeneration of the biosensing surface is highly repeatable, which may improve the quantification accuracy. The biosensing platform was very useful in the evaluation of kinetic constants of DNA hybridization using the proposed theoretical basis. The novel biosensing platform presented here could not only provide a simple, cheap, fast, and robust technique as an alternative to currently available approaches, particularly for early cancer detection, point-of-diagnosis, and on-site analysis but it also shows promising application on the detection of protein–protein and DNA–protein real-time interactions. In addition, this setup can be directly integrated with microelectronics and microfluidics systems to gain advantages in miniaturization and multiplex detection because of the multicolor resolution of QDs.

Acknowledgments

This research was supported by the 863 National High Science and Technology Development Programs (2009AA06A417), Major projects on control and rectification of water body pollution (2008ZX07313-007), and Postdoctor Science Foundation (20080440035).

References

Abel, A.P., Weller, M.G., Duveneck, G.L., Ehrat, M., Widmer, H.M., 1996. Anal. Chem. 68, 2905–2912.
Bhatia, S.K., Shrive-Lake, L.C., Prior, K.J., Georger, J.H., Calvert, J.M., Bredehorst, R., Ligler, F.S., 1989. Anal. Biochem. 178, 408–413.
Chan, W.C.W., Nie, S.M., 1998. Science 281, 2016–2018.
Ebersole, R.C., Miller, J.R., Moran, J.R., Ward, M.D., 1990. J. Am. Chem. Soc. 112, 3239.
Fang, X., Liu, X., Schuster, S., Tan, W., 1999. J. Am. Chem. Soc. 121, 2921.
Fisher, R.J., Fivash, M., Casas-Finet, J., Erickson, J.W., Kondoh, A., Bladen, S.V., Fisher, C., Watson, D.K., Papas, T., 1994. Protein Sci. 3, 257–266.
Gao, Y., Wolf, L.K., Georgiadis, R.M., 2006. Nucleic Acids Res. 34 (11), 3370–3377.
Golden, J.P., Saaski, E.W., Shriver-Lake, L.C., Anderson, G.P., Ligle, F.S., 1997. Opt. Eng. 36, 1008–1013.
Li, D., Zou, X., Shen, Q., Dong, S., 2007. Electrochem. Commun. 9, 191–196.
Michalet, X., Pinaud, F.F., Bentolila, L.A., Tsay, J.M., Doose, S., Li, J.J., Sundaresan, G., Wu, A.M., Gambhir, S.S., Weiss, S., 2005. Science 307, 538–544.
Myszka, D.G., 1997. Curr. Opin. Biotechnol. 8, 50–57.
Leung, A., Shankar, P.M., Mutharasan, R., 2007. Sens. Actuators B 125, 688–703.
Long, F., He, M., Shi, H.C., Zhu, A.N., 2008a. Biosens. Bioelectron. 23, 952–958.
Long, F., Shi, H.C., He, M., Zhu, A.N., 2008b. Biosens. Bioelectron. 23, 1361–1366.
Okahata, Y., Kawase, M., Niikura, K., Ohtake, F., Furusawa, H., Ebara, Y., 1998. Anal. Chem. 70, 1288–1296.
Peterson, A.W., Heaton, R.J., Georgiadis, R.M., 2001. Nucleic Acids Res. 29 (24), 5163–5168.
Peterson, A.W., Wolf, L.K., Georgiadis, R.M., 2002. J. Am. Chem. Soc. 124, 14601–14607.
Rant, U., Pringsheim, E., Kaiser, W., Arinaga, K., Knezevic, J., Tornow, M., Fujita, S., Yokoyama, N., Abstreiter, G., 2009. Nano. Lett. 9 (4), 1290–1295.
Rant, U., Arinaga, K., Scherer, S., Pringsheim, E., Fujita, S., Yokoyama, N., Tornow, M., Abstreiter, G., 2007. PNAS, 17364–17369.
Resch-Genger, U., Grabolle, M., Cavaliere-Jaricot, S., Nitschke, R., Nann, T., 2008. Nat. Methods 5 (9), 763–775.
Sassolas, A., Leca-Bouvier, B.D., Blum, L.J., 2008. Chem. Rev. 108, 109–139.
Sukhanova, A., Devy, J., Venteo, L., Kaplan, H., Artemyev, M., Oleinikov, V., Klinov, D., Pluot, M., Cohen, J.H., Nabiev, I., 2004. Anal. Biochem. 324, 60–67.
Tedeschi, L., Domenici, C., Ahluwalia, a., Baldini, F., Mencaglia, A., 2003. Biosens. Bioelecron. 19, 85–93.
Watterson, J.H., Piunno, P.A.E., Wust, C.C., Krull, U.J., 2000. Langmuir 16, 4984–4992.
Yu, F., Yao, D., Knoll, W., 2004. Nucleic Acids Res. 32, e75.
Zeng, J., Almadidy, A., Watterson, J., Krull, U.J., 2003. Sens. Actuators B 90, 68–75.
Zhang, Y, Wang, Y., Wang, H., Jiang, J.H., Shen, G.L., Yu, R.Q., Li, J., 2009. Anal. Chem. 81, 1982–1987.
Zhou, D., Ying, L., Hong, X., Hall, E.A., Abell, C., Klenerman, D., 2008. Langmuir 24, 1659–1664.